Transactions, SMiRT-24
BEXCO, Busan, Korea - August 20-25, 2017
Division VII

ANALYSIS OF THE CONSEQUENCES OF AN AIRPLANE CRASH ON AN UNDERGROUND RADIOACTIVE WASTE STORAGE BUILDING PART I: STRUCTURAL ANALYSIS

A. Nykyforchyn[1], M. Miloshev[2], M. Kostov[3], P. Steiner[4], J.-U. Klügel[5]

[1] Senior Engineer, NPP Gösgen-Däniken, Däniken, Switzerland
[2] Chief Expert, Risk Engineering, Sofia, Bulgaria
[3] Director, Risk Engineering, Sofia, Bulgaria
[4] Senior Engineer, NPP Gösgen-Däniken, Däniken, Switzerland
[5] Director, NPP Gösgen-Däniken, Däniken, Switzerland

ABSTRACT

Consequences of a hypothetical crash of a military aircraft F-4 onto the underground radioactive waste storage were investigated. The primary objective of the first step of this study was to evaluate the amount of fuel that penetrates the roof of the storage building. The integral simulation approach was used to analyse the impact of the airplane on the RC roof slab covered with asphalt concrete layer. A detailed finite element model of the airplane was developed, which included fuselage, wings, engine and non-structural parts. In order to evaluate the dispersion and penetration of fuel it was modelled as SPH particles. The results were compared to those with the rigid fuel model by finite elements. The whole aircraft model was validated by comparing the rigid wall analysis with the SNL full scale test onto the concrete wall.
Sensitivity analyses of the penetrated amount of fuel on various model parameters were performed. They included the influence of the impact location and angle as well as effect of the material model of concrete, reinforcement, asphalt concrete and the aircraft. Incorporation of the asphalt concrete layer in the structural model has a significant impact on the roof damage, airplane residual velocity and the fuel penetration.
In addition, the area of the penetration hole was calculated, which is important for the subsequent fire analyses. However, the effective area is reduced by the airplane debris stuck, which evaluation is limited by the erosion of elements.

INTRODUCTION

NPP Gösgen has evaluated a hypothetical MAC impact on the underground low and intermediate level radioactive waste (LLW and ILW) storage buildings and the resulting kerosene fire and radiological consequences. The MAC is expected to create a breach (a “hole”) in the roof of the buildings and project debris and kerosene from the aircraft into the buildings. The buildings contain stacks of stainless steel (SS) barrels filled with bituminized radioactive wastes. The key questions here are the impacts of the kerosene fire and the potential damage to the LLW and ILW waste barrels that could lead to a bitumen fire and consequent release of the radioactive materials embedded in the bitumen.

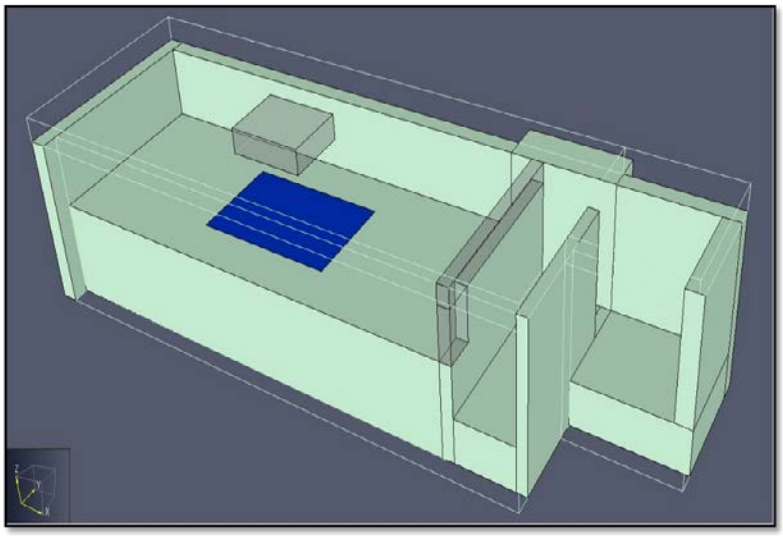

Figure 1: Configuration of the ILW building and of the compartment considered for the fire analysis

The evaluations of the mechanical and thermal impacts of a MAC on the ILW and LLW buildings and their radiological consequences have been performed in two stages. First a detailed, realistic structural analysis of the impact of a MAC on the ILW building was performed providing best estimate analysis of the hole size and shape, debris amount, kerosene mass entering the building, and the resultant speeds of aircraft and debris. This first part of the study is presented in the current paper. The results of these analyses provided the input for the second part of the study, which is detailed fire analyses based on a Computational Fluid Dynamics (CFD) methodology, which are discussed in the other paper.

The current paper presents assessment of the structural capacity of a reinforced concrete (RC) underground ILW building for the consequences of impact with F-4 Phantom military jet by the missile-target interaction (MTI) method. Detailed finite element (FE) models of the missile (the airplane) and the structure (target) have been developed. The FE model of the airplane is validated by performing finite element impact analyses into rigid wall and moveable concrete block. The output results are compared with data, obtained from full-scale impact test performed at the SANDIA National Laboratory. The target structure is covered by a layer of asphalt. It is included in the model because it acts as an energy dissipation layer and increases the structural capacity in case of high velocity impact. A number of impact analyses are performed considering asphalt properties, defined for different temperatures and strain rates. The parameters which are compared as a result are the perforation areas of the target's top slab and the corresponding fuel amounts which penetrate into the structure.

MODELLING OF THE AIRPLANE CRASH

Methodology

The impact analyses were performed by missile-target interaction (MTI) method with the software package LS-Dyna. Impact force of the airplane causes local damage of the building structure. When the critical strain of the finite elements of the structure has been reached, these elements were assumed to failed and were deleted from the structure. Consequent erosion of the structure elements resulted in the penetration and further full perforation building roof, creating a hole. Further penetration of the structural elements of the airplane and the fuel through the hole was analyzed. The analysis was stopped when no more damage of the building occurred and no more fuel was penetrating through the opening.

Airplane Modelling and Validation

Two FE models of the aircraft are created, whereas two fuel models are considered – rigid fuel model and Smooth Particle Hydrodynamics (SPH), see LSTC (2016). The approach for modelling aircraft fuel using SPH is described by Kostov et al. (2015). The rigid fuel model refers to the case where the mass of the fuel is taken into account by increasing the mass density of the structural parts of the fuel tanks. Apart from the fuel, both FE models are the same and are built entirely of shell elements. The material properties were assumed to be those of a typical aluminium alloy, while the bilinear kinematic hardening model (MAT003) was used. The dynamic increase of the material strength due to strain rate effects is considered by using the Cowper-Sydmonds strain rate model. The material properties of the SPH correspond to water.

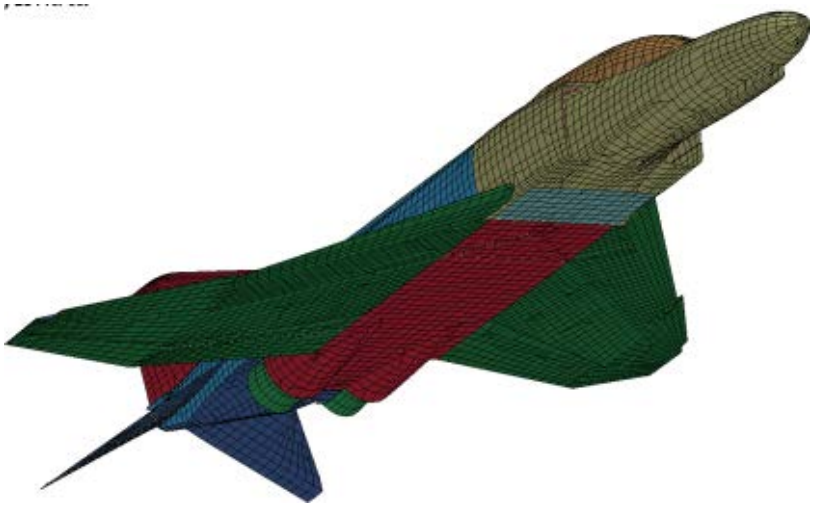

Figure 2. FE model of a F4 Phantom

The airplane models were validated by performing impact analyses into rigid wall and concrete block, which are simulated conditions of the SANDIA Labs full scale test, see Sugano et al. (1993). The purpose of the test was to obtain the load-time function for impact of F-4 Phantom aircraft into an essentially rigid wall. A flyable F-4D was acquired and used for the purpose. The total mass of the aircraft was 19 t including 4.8 t of water (to simulate fuel) and 1.5 t mass of the sleds and the solid rockets for propulsion. The plane was accelerated against the target, which was a reinforced concrete block with mass 469 t. The concrete block was placed on air bearings in order to avoid friction with the supporting structure. Various measuring devices were attached to the concrete block in order to record its response. The impact speed of the aircraft was 215 m/s and the impact direction was normal to the surface of the target.

The mass distribution of the airplane model complies with the SANDIA test conditions. In the impact model the concrete block is not supported in direction of impact in order to match the experiment set-up. Pictures from the impact analyses are shown in Figure 3.

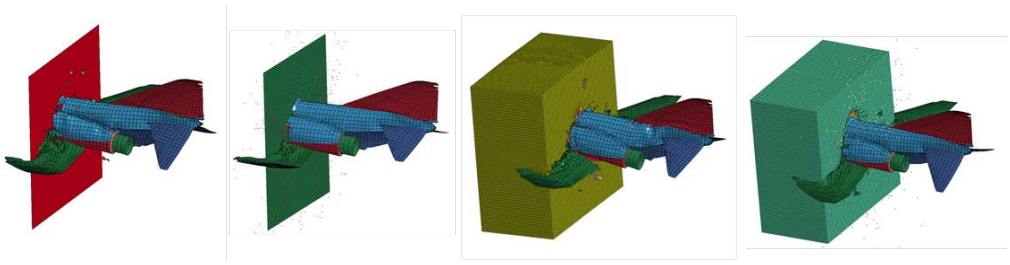

Figure 3. Impact of the FE airplane models into rigid wall and concrete block

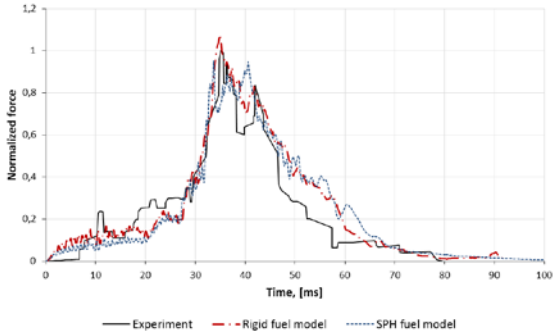

Figure 4. LTFs from analyses into rigid wall

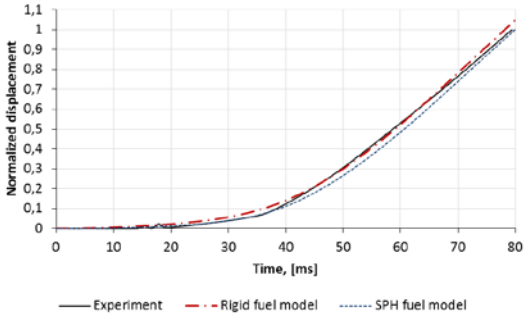

Figure 5. Displacement of the concrete block

The normalized load-time functions (LTF), obtained from the FE analyses into rigid wall are compared to the load-time function obtained from the SANDIA experiment in Figure 4. Very good match between the load curves from the experiment and from the FE analysis with rigid fuel model is observed, especially at the peak force values. The load curve calculated by the FE analysis with SPH fuel model slightly differs from the experimental one in the peak values but the overall shape is similar. The deviations at the peak values are attributed to the interaction between the SPH particles and the aircraft structure and the rigid wall. Similarly, the forces resulting from the analyses into the concrete block (not shown here) demonstrate good agreement with the experiment. Figure 5 shows comparison of the displacements of the concrete block. Apparently, the displacement histories obtained from the numerical analyses match very well the experimental one. Other parameters such as the momenta and the velocities of the concrete block are also found to agree very well with the corresponding experimental measurements.

Impact Target Model

The model of the target structure is shown in Figure 6. In addition to the RC structure of the building, the soil surrounding the underground structure, as well as the asphalt layer on top are also modeled. The RC structure and the asphalt were modelled with 3D solid elements.

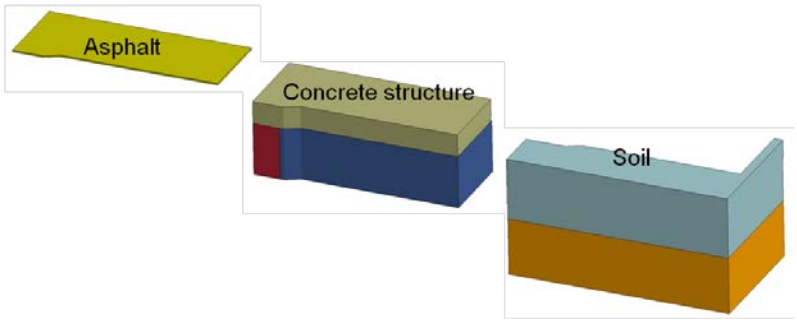

Figure 6. FE model of the target structure

The concrete is modeled by the Continuous Surface Cap Model (MAT159 CSCM Concrete in LS-Dyna). The CSCM model parameters were calculated based on the concrete compression strength, aggregate size and density. The essential erosion coefficient is a fitting parameter, obtained by matching the numerical simulation results of the VVT impact tests to the test results (residual velocity and the concrete damage pattern). Plastic Kinematic (LS-Dyna MAT003) model is used of the reinforcement.

Material Models of the Asphalt Concrete

The material model of Drucker-Prager (DP, MAT193 in LS-Dyna) was used for the asphalt concrete material. The use of this material model for asphalt is reported by Seibi (2001) and Zhang et al. (2013). The main parameters of the DP material are the internal friction angle ϕ, the cohesion c and the shear modulus G. These parameters are defined considering literature resources. Additionally, the asphalt is modeled with the Karagozian & Case concrete model (KCC, MAT072R3 in LS-Dyna) in an attempt to capture its contribution to the structural behavior.

The material properties of asphalt depend on the temperature and the strain rate, i.e. the speed of loading. A relation between the asphalt compressive strength, the temperature T and the strain rate $\dot{\varepsilon}$ is published by Erkens and Poot (2000):

$$f_c = -108\left(1 - \frac{1}{1+\left(\dot{\varepsilon}.e^{-86.3+\frac{24260}{T}}\right)^{0.32}}\right) \quad (1)$$

Plots of the compressive strength of asphalt as function of strain rate for different temperatures, computed using formula is (1) shown in Figure 7.

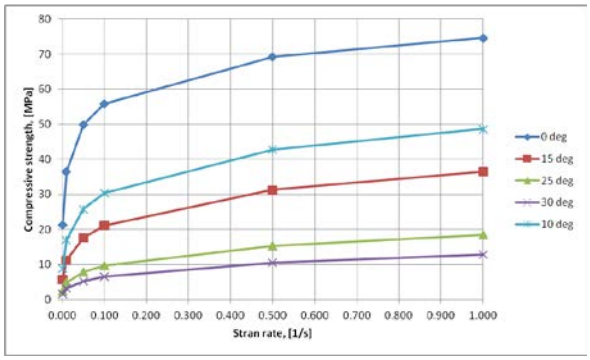

Figure 7. Asphalt compressive strength vs. strain rate

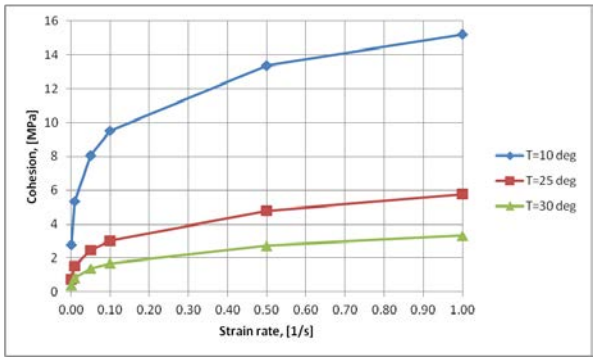

Figure 8. Cohesion vs. strain rate

Formula (2) relates the asphalt compressive strength, the cohesion and the angle of internal friction (see Pellinen et al. (2004)):

$$f_c = \frac{2.c.\cos\phi}{1-\sin\phi} \quad (2)$$

By using formula (2) one can compute the cohesion c for given angle of internal friction ϕ and compressive strength which, in turn, can be defined for given strain rate and temperature using formula (1). The material properties of the asphalt are defined for three temperatures – 10^{O}C, 25^{O}C and 30^{O}C. The angles of internal friction which correspond to these temperatures are taken from literature resources (Hopkins (2005) and Cox (1960)) as follows: $\phi = 26^0$ (for T=10^0C and T=25^0C) and 35^0 (for T=30^0C). Plots of the cohesion as function of strain rate for the temperatures of interest are shown in Figure 8.

The shear moduli of the asphalt required for the input of the DP material are calculated from the moduli of elasticity. The latter are adopted from the paper of Erkens and Poot (2000) which contains stress-strain curves in compression, experimentally obtained by testing asphalt specimens under different strain rates and temperatures. The elasticity and shear moduli for the three temperatures of interest and strain rate 1.0/s are given in Table 1.

Table 1. Computed elasticity and shear moduli

	T=10^{0}C	T=25^{0}C	T=30^{0}C
E, [MPa]	16320.74	5160.5	1479.6
G, [MPa]	6277.208	1984.808	569.0769

The KCC model is used as an alternative for the asphalt concrete with the intention to account for its tension strength. Using the KCC model, the asphalt layer is modelled as concrete with compressive strength 48 MPa. This compressive strength corresponds to strain rate $\dot{\varepsilon}$ = 1 and temperature 10^{0}C as seen in Fig. 9. The KCC model is chosen for the asphalt concrete model because it allows direct input of the tensile strength, i.e. it is not computed from the compressive strength through the material model relations. The static tensile strength is assumed to be 2.4 MPa after Kennedy (1983). The increase of the tensile strength due to strain rate effects is considered by dynamic increase factor (DIF), computed according to formula (3) published by Wu and Liu (2015).

$$DIF = 1.86 + 0.1432 \log_{10} \dot{\varepsilon} \text{ for } \dot{\varepsilon} \le 15 s^{-1} \quad (3)$$

For strain rate $\dot{\varepsilon}$=1 the DIF is obtained to be 1.86. The values of the tensile and compressive strength are defined for strain rate $\dot{\varepsilon}$=1 and no further dynamic increase is considered by the material model.

Analysis setup

Four analyses are performed using material parameters of asphalt DP model for temperatures 10^{O}C, 25^{O}C and 30^{O}C, as well as the KCC model. The approach for computing the parameters is described above. Strain rate $\dot{\varepsilon}$=1 is considered although higher values are reached during high velocity impact. The reason is that the investigations in the literature resources which are reviewed assume the use of asphalt concrete for transportation purposes where the strain rates in general are much lower and the extrapolation of the results may not be accurate. The mass of the airplane is assumed to be 20 t in order to comply with the requirements of NS-G 1.5 (2003).

FUEL PENETRATION RESULTS

Damage and perforation area

The analysis results which are compared are the area of the perforation of the RC plate and the mass of fuel which penetrates through the perforation. The latter parameter is important for assessment of the fire consequences inside the structure.

The nominal perforation area is computed by projecting the contour of the perforation onto a horizontal plane. For the mean annual asphalt temperature of 10°C the nominal perforation area of 8.2 m^2 was calculated.

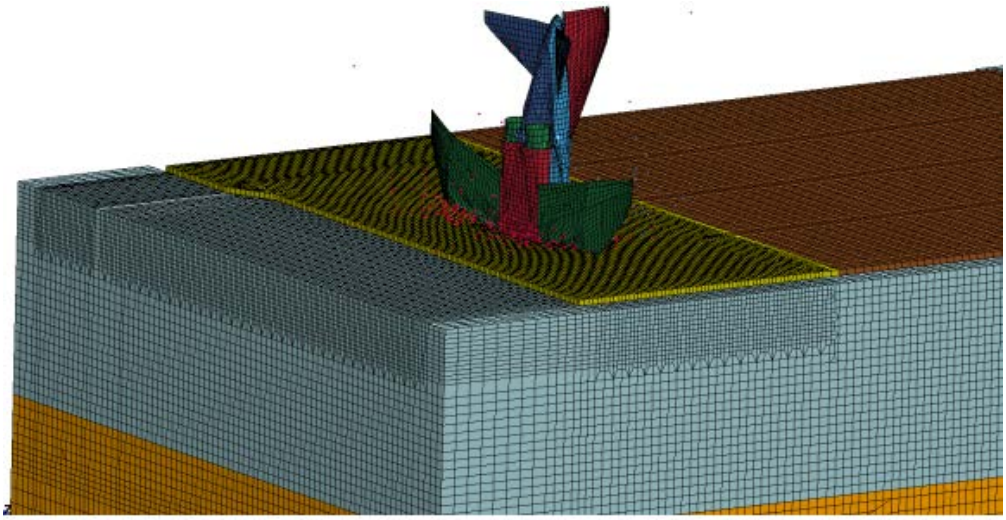

Figure 9. Impact of F4 onto the ILW building

In all analysis cases the airplane gets stuck into the plate, it does not completely penetrate through it. Therefore, the effective perforation area, which is significant for the oxygen supply for the kerosene fire, is reduced by the stuck airplane structure, hanging concrete debris as well as the eroded debris of the roof and the airplane.

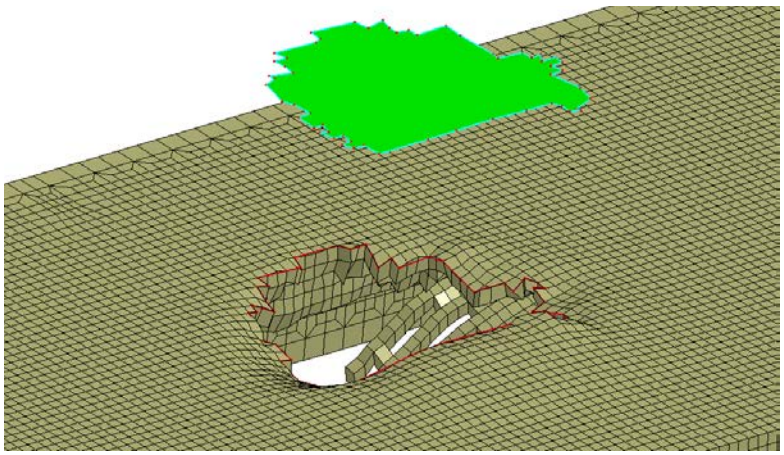

Figure 10. Perforation area calculation

Fuel Penetration

The amount of fuel is estimated by measuring the mass of the SPH particles which penetrate inside. It can be seen that most fuel particles dispense outside the building. The fuel particle reflection by the eroded debris could not be considered.

The perforation areas and the corresponding fuel masses are summarised in **Table 2**.

Table 2. Summary of the analysis results

Asphalt model	DP model at 10^0C	DP model at 25^0C	DP model at 30^0C	KCC model
Perforation area, m^2	8.2	8.6	8.8	7.4
Fuel mass, kg	480	860	715	850

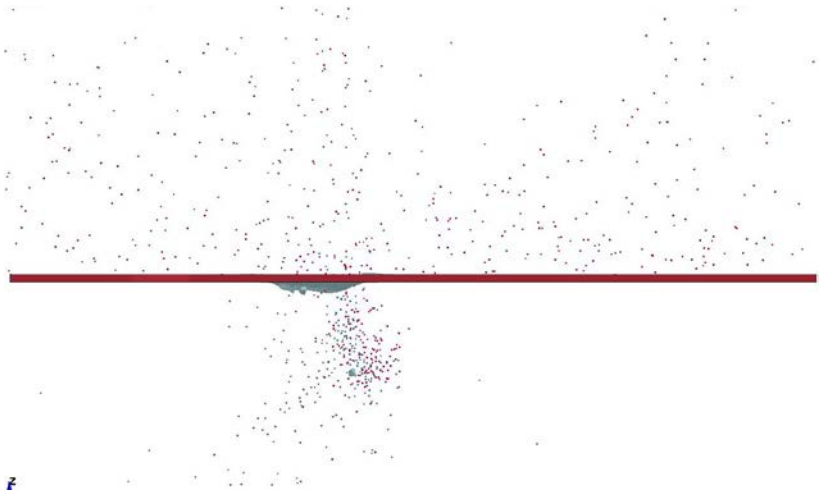

Figure 11. SPH fuel particles outside and inside the ILW building

SENSITIVITY ANALYSES

Penetration Position

The penetration position in the base case analysis was chosen in the middle of the roof of the ILW building. This slab area with the largest distance between the supporting walls was assumed to be a worst case position. To verify this assumption, another impact analysis was performed on the roof of the LLW building, where the walls of the compartments are closer, Figure 12 (left).

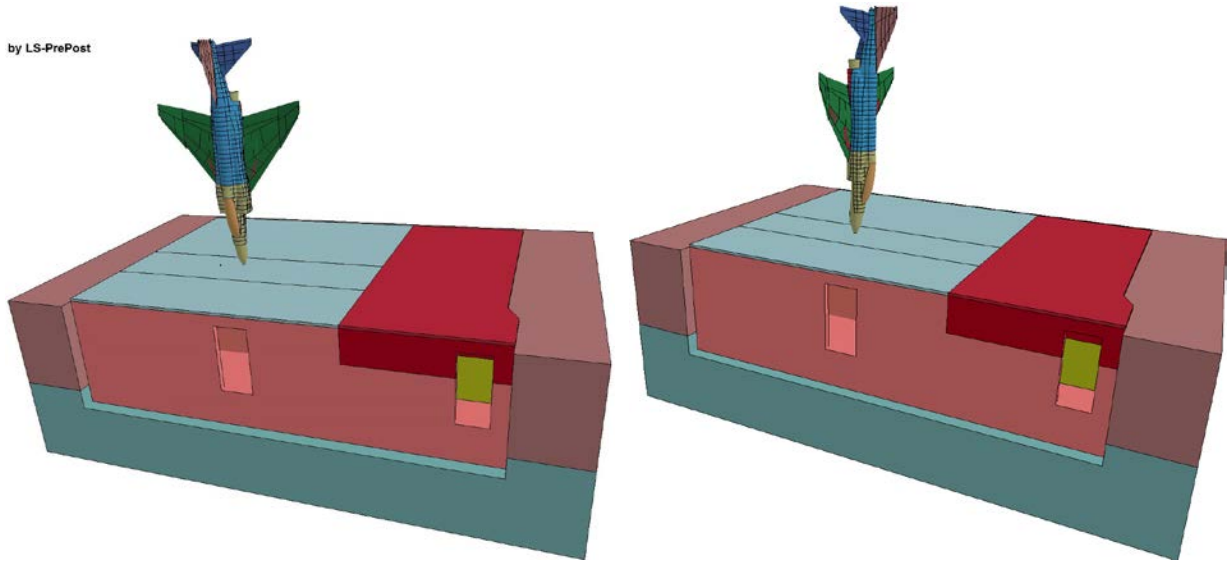

Figure 12. Impact of F4 onto the LLW building: two cases of rotational position

The results showed the perforation area that is similar to that of the base case study of the ILW building. However, the perforation hole is less blocked by the debris than for the ILW building. This contributes to a 2.3 times higher amount of penetrated fuel compared to the base case.

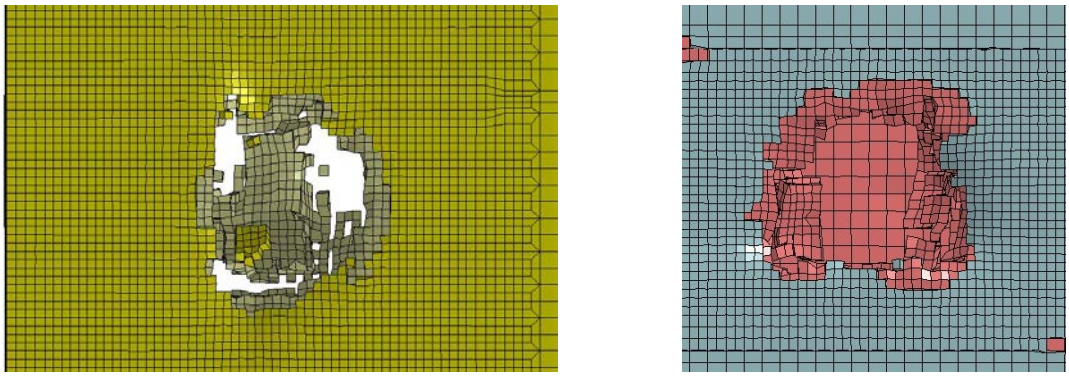

Figure 13. Perforation area of the ILW (left) and LLW (right) buildings

In the second case study, the airplane was rotated 90° in respect to the impact axis, so that the wings of the airplane hit the compartment walls, Figure 12 (right). The results show that this have no effect on the overall impact resistance, so that the amount of penetrated fuel does not significantly change.

Thus there is no positive effect of having more walls, supports or putting more reinforcement unless the penetration can be arrested before the full perforation. The hard impact has practically no bending damage mechanism, which can benefit from the wall spacing. On the contrary the higher flexibility of the roof with a large wall distance may result in additional energy dissipation due to bending deformation.

Material Models

To evaluate the sensitivity of the analysis results to the material models of the airplane, the bilinear material model with the Cowper-Sydmonds strain rate parameters was substituted by the Johnson-Cook constitutive model (MAT015 in LS-DYNA). While the Johnson-Cook model is computationally more expensive, it provides a better fit of the strain stress relationship.
The flow stress and the fracture strain are determined from

$$\sigma = (A + B\,\varepsilon^{n})\left(1 + C\,ln\left(\frac{\dot{\varepsilon}}{\dot{\varepsilon}_0}\right)\right) \qquad \epsilon_f = \left(D_1 + D_2\, e^{D_3\frac{p}{\sigma}}\right)\left(1 + D_4\, ln\left(\frac{\dot{\varepsilon}}{\dot{\varepsilon}_0}\right)\right) \tag{1}$$

The JC model parameters for the aluminium 2024-T3 alloy C = 0.0083, D_1=0.13, D_2=0.13 D_3=-1.5, D_4=0.07 were taken from Lesuer (2000). The rate independent parameters A = 300 MPa, B = 360 MPa, n = 0.25 and ε_{fmin} = 0.2 were obtained by fitting the strain-stress curve of 2024-T3 alloy at low strain rate.

The analysis results show no evident difference of the penetration hole size. The resultant amount of penetrated fuel is nearly 20% lower.

Impact Velocity

The design impact velocity of 215 m/s is very high and hard to achieve during the controlled impact. Therefore, several cases were studies with lower impact velocities. The results of the first case with the impact velocity of 200 m/s showed a similar perforation hole area. Contrary to the expectation, the amount of penetrated fuel was 1.6 times higher. This can be caused by the fact, that at a higher impact velocity the fuel tanks got damaged (burst) before the penetration occurs, so that the bigger amount of fuel remains outside the building.

Analysis Parameters

It has been found that the analysis results are rather sensitive to the contact definition, SPH definition as well as the LS-DYNA solver version. One of the biggest uncertainty in the current study is caused by the erosion of the elements of the airplane structure, the asphalt layer and the RC structure after the critical strain has been exceeded. Firstly, the debris (destroyed aluminium parts or concrete particles) are partially getting stuck over the undamaged structure, so that the impact area is continuously increasing. Since the damage mechanism is the punching of the concrete slab, the damage level is highly dependent on the impact area. Spreading of the impact force over a large area might beneficial at low impact energy if the full perforation of the wall can be avoided. However, if the impact force is sufficiently high, a larger impact area might result in a higher actual perforation area than those calculated with element erosion.

CONCLUSION

The FE model of the airplane which is created for the purposes of the MTI analyses is validated by comparison of numerical impact simulations to available test data. The impact force agrees very well with the experimental results as seen in Figure 4. Conclusion can be drawn that the mass and stiffness distribution of the missile are well captured by the FE model and it is suitable for performing MTI analyses.

The impact analyses of the RC target are performed considering different models of the asphalt layer (DP and KCC) which is laid over it. The asphalt is introduced as an energy dissipation layer during the high velocity impact. As shown above, the asphalt compressive strength and cohesion increase with increase of strain rate and decrease with increase of temperature. The perforation areas summarized in Table 2 show similar perforation areas obtained from the analyses whereas the smallest perforation area corresponds to the setup with KCC model for the asphalt. A tendency is observed, that the perforation area increases with increase of the temperature, which corresponds to decrease of the cohesion of asphalt. In other words, a correlation between the asphalt properties and the damage is established.

The measured fuel masses do not follow this tendency but credit should be given to the fact that the penetrating fuel depends not only on the damage of the target but also on the crushing pattern of the airplane. The fact that the aircraft does not fully penetrate into the structure implies that the internals will be subjected only to impact of small structural debris.

It has been found that the analysis results are highly sensitive to the impact position and less sensitive to the type of the material model of the airplane structure. The restraint of the fuel penetration by concrete and airplane debris could not be taken into account due to the failed element erosion in the FE model.

REFERENCES

Cox., B. (1960) “The effect of asphalt content and temperature on the triaxial properties of an asphalt concrete mix”, *Thesis*, Georgia Institute of Technology.

Erkens, S., Poot, M. (2000) “Determining and modeling asphalt concrete response”, HERON, V.45, No.3.

Hopkins, T. at al. (2005). ”Bearing capacity analysis and design of highway base materials reinforced with geofabrics”, Kentucky transportation center.

IAEA, NS-G 1.5, “External events excluding earthquakes in the design of nuclear power plants”, 2003.

Kennedy, T. (1983) “Tensile characterization of highway pavement materials”, Center of transportation research, The university of Texas at Austin.

Kostov, M., Miloshev, M., Nikolov, Z., Klecherov, I. (2015) “Non-structural mass modelling in aircraft impact analysis”, *Proc. 23d Conf. Structural Analysis in Reactor Technology*, Manchester, UK.

Lesuer.D. R:(2000) "Experimental Investigationsof Material Models for Ti-6Al-4V Titanium and 2024-T3 Aluminum". Report DOT/FAA/AR-00/25. Lawrence Livermore National Laboratory.

LSTC (2016). “LS-Dyna Keyword User’s Manual Volume I”, LS-Dyna R9.0.

Pellinen, T.K. et al. (2004) “Characterization of hot mix asphalt with varying air voids content using triaxial shear strength test”, CAPSA, Sun City, South Africa.

Seibi, A. (2001) “Constitutive relations for asphalt concrete under high rates of loading”, Transportation research record, *Journal of the transportation research board*.

Sugano, T. et al. (1993) ”Full-scale impact test for evaluation of impact force”, *Nuclear Engineering and Design*, UK, 140, 373-385.

Wu, J., Liu, X. (2015). “Performance of soft-hard-soft (SHS) cement based composite subjected to blast loading with consideration of interface properties”, *Frontiers of structural and civil engineering.*

Zhang, Y. et al. (2013). “A comprehensive characterization of asphalt mixtures in compression”, Southwest Region University Transportation Center, Texas A&M Transportation Institute.